




cambridge.org/mrf

Nitika , Jaswinder Kaur and Rajesh Khanna

Department of Electronics and Communication Engineering, Thapar Institute of Engineering and Technology, Patiala, Punjab, India

Research Paper

Cite this article: Nitika, Kaur J, Khanna R (2023). Exploration of adulteration in common raw spices using antenna-based sensor. *International Journal of Microwave and Wireless Technologies* **15**, 1117–1129. <https://doi.org/10.1017/S175907872200112X>

Received: 10 June 2022
Revised: 21 September 2022
Accepted: 22 September 2022

Key words:

Antenna sensor; dielectric permittivity; high sensitivity; *Q*-factor; reflection coefficient

Author for correspondence:

Nitika,
E-mail: nnitika_phd19@thapar.edu

Abstract

The ability of food products to store and dissipate electromagnetic energy is determined by the material's dielectric properties. In relation to this phenomenon, a non-destructive technique is presented for food evaluation based on the shift in resonant frequency and reflection coefficient magnitude value of the proposed slot-loaded microstrip line-fed antenna-based sensor caused by the change in dielectric properties of the food material. In this work, a miniaturized antenna sensor of $10 \times 10 \text{ mm}^2$ size comprised of a dielectric substrate FR-4 with permittivity (ϵ_r) = 4.4 having ground plane at the bottom and a radiating element at the top is designed to operate at 13.3 GHz. Three samples of spices, i.e. red chilli powder, black pepper powder, and turmeric powder, are considered for quality monitoring whose relationship in terms of reflection coefficient, resonant frequency, and dielectric permittivity at 13.17, 12.61, and 13.09 GHz respectively is analyzed. Further, second-order polynomial model is derived to predict dielectric permittivity of the material under test with high accuracy. The experimental procedure of this proposed sensor is based upon the interaction of the sample food materials with the electromagnetic field owing to shift in resonant frequency as a function of dielectric permittivity of the samples. The proposed antenna sensor has a *Q*-factor of 409, showing significantly high sensitivity of 280 MHz with 98% accuracy and standard deviation less than the difference between unadulterated and adulterated values, giving resolution high enough to distinguish adulteration with an acceptable statistical accuracy.

Practical application: The results of this study recommend that the proposed antenna-based sensor with novel configuration can be used for industrial purposes as it is having a relatively less complex procedure for determining the extent of adulteration in solid food materials with high accuracy.

Introduction

One of the basic needs for every living being is food which is composed of carbohydrates, water, fats, and proteins; which are consumed by humans for nutritional purpose. In this present era, food adulteration has become a serious threat for the society especially in developing countries as people are opting unfair means to earn profit [1, 2]. Food adulteration is defined as the process in which the quality of food material is degraded either by adding material with inferior quality, by extracting valuable ingredient, or by adding low-cost materials [3, 4]. In addition to this, various products are naturally contaminated due to aging, industrial inventions, and during natural calamities, which not only degrade the quality of food materials but have dangerous effects on different living beings and natural vegetation [5].

Since birth every citizen is entitled to consume wholesome food, so it is requisite to track adulterated food products before consuming it. However, it is impossible to check the quality of food materials to ensure its nutritive value only on the basis of visual inspection, especially when adulterant resembles the base product [6, 7]. There are certain properties of the material that are associated with each raw material, especially electric properties like dielectric permittivity that could be examined to check the adulteration in food samples to assure its quality [8, 9]. When two materials possessing different values of permittivity are mixed together then it results into third effective permittivity whose value lies in between the two parental values, from which some sight of adulteration can be traced [10]. The microwave sensors have the ability to sense the permittivity variations which results in the change of electromagnetic field distribution upon interaction with materials having different dielectric properties [11]. In addition, microwave technology provides non-destructive and non-invasive environment for material testing [12, 13]. Hence, microwave characterization techniques have found a wide range of applications in the field of health, agriculture, and food industries [14–16].

There are a number of microwave techniques, among which the resonant methods are considered to be more reliable and accurate, since these methods involve the testing of a material at single or discrete frequencies [17, 18]. The devices engaged for the characterization purpose of the materials are referred as sensors, as they have the ability to sense the change in material

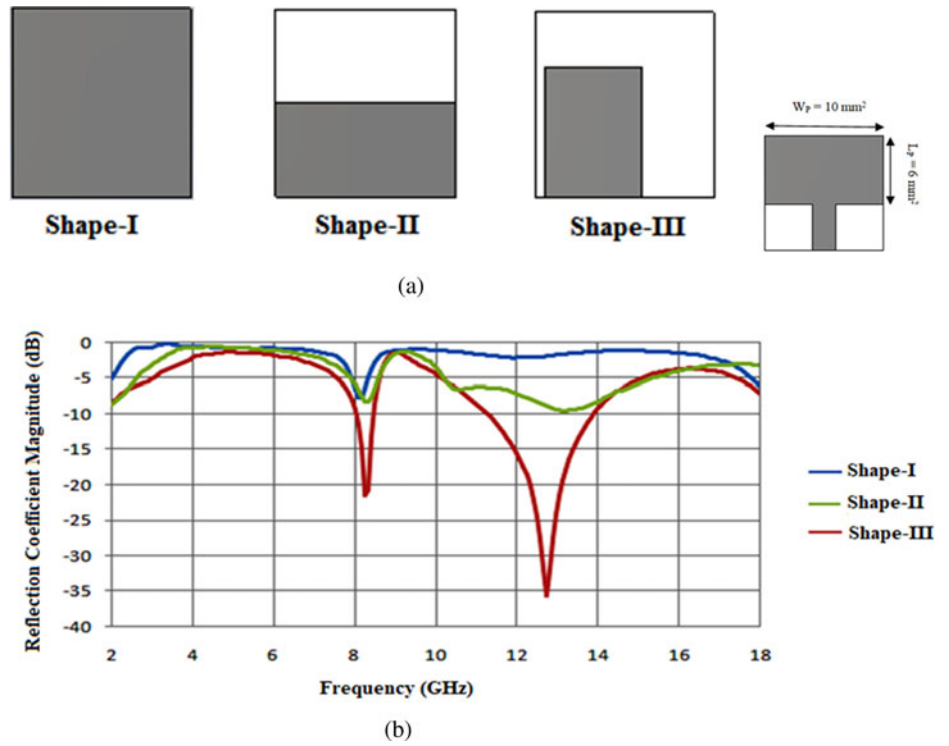


Fig. 1. (a) Geometrical layout for different ground plane structures. (b) Reflection coefficient magnitude corresponding to different ground plane structures.

properties on the bases of variation in sensor response such as resonant frequency, reflection coefficient, quality factor, etc. [19]. There are a number of resonant sensors that are available in the literature; the planar technology is more attractive in the current scenario because of its compact size, low cost, and less performance time with easy data interpretation [20]. The propagation of electromagnetic field determines the dielectric properties to reveal the parameters of food object using microwave sensor are

mainly through three measurement modes: reflection, transmission, and resonance [21, 22].

Nowadays, various microwave sensor technologies are merchandized for detecting sugar, salinity, moisture content, humidity, etc. For instance, a microstrip patch antenna proposed for measuring salt and salinity in water has been reported in literature review [23]. A waveguide probe and reflection method was introduced to measure complex permittivity of a phantom of

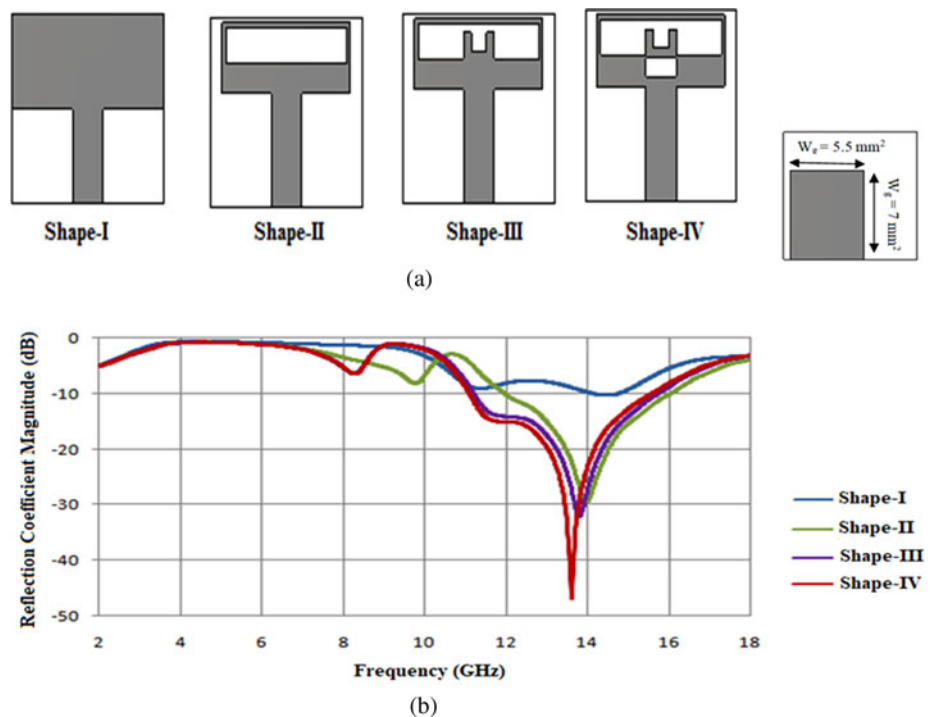


Fig. 2. (a) Geometrical layout for different radiating patch structures. (b) Reflection coefficient magnitude corresponding to different radiating patch structures.

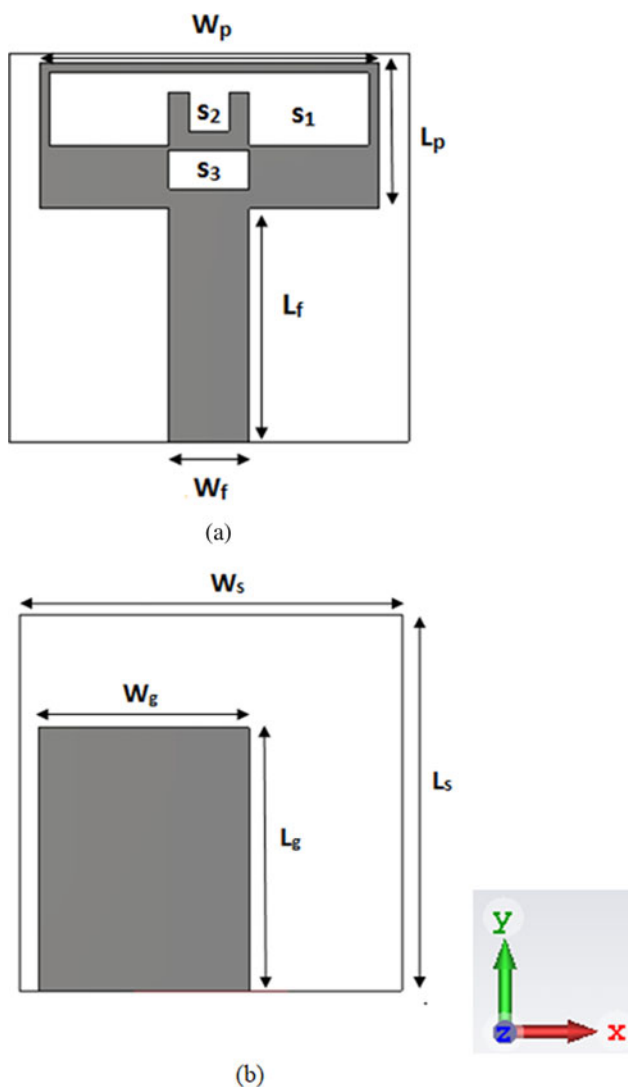


Fig. 3. Geometrical layout of slot-loaded proposed antenna sensor in CST Microwave Studio. (a) Top view. (b) Bottom view.

Table 1. Geometrical parameters of the proposed microstripline-fed antenna sensor

Parameters	Values (mm)
Patch	$L_p = 3.75$; $W_p = 8.5$
Ground	$L_g = 7$; $W_g = 5.5$
Slots	$S_1 = 1.875 \times 8$; $S_2 = 1 \times 1$; $S_3 = 1 \times 2$

biological muscle tissue [24]. Further for determining the moisture in oil palm fruits, a waveguide technique has been proposed [25]. For humidity sensing, a polymer-loaded ultrawide band RF identification sensor has been introduced [26]. Apart from these, many antenna sensors have been designed for air quality monitoring, medical checkup, food analysis, etc. [27–29]. However, all these methods are considered to be time-consuming with some complex procedure and complicated data interpretation, which require skilled operators to handle and use these microstrip-based antenna sensors. Therefore, for food evaluation, novel,

miniaturized, and cost-effective planar resonant RF sensor with improved sensitivity and considerable quality factor (*Q*-factor) is required for adulteration detection which can potentially be used as a substitute against existing fiber optic and chemical-based methods [30, 31].

In this article, a miniaturized slot-loaded microstrip line-fed antenna-based sensor is deployed for detecting adulteration in some common spices such as red chilli powder adulterated with brick powder, black pepper powder adulterated with papaya seeds, and turmeric powder adulterated with artificial yellow color. The detection of adulteration is observed against the variation in reflection coefficient magnitude and shift in resonant frequency depending upon the amount of adulterant that is mixed with the pure sample which is further represented in graphical form to show the linear variation. At last, to focus on associated merits of the chosen sensor, the performance parameters of proposed antenna sensor are compared with the earlier work presented in the literature. It is recognized that the proposed microstrip antenna sensor has high sensitivity with good quality factor compared to other available sensors. Further, a small value of standard deviation gives resolution high enough to distinguish adulteration with an acceptable statistical accuracy.

Materials and methods

Design and characterization of proposed antenna-based sensor

Step-by-step evolution of proposed design

The step-by-step evolution of the layout of antenna sensor design to achieve desired result is represented in this section. The simulation and parametric optimization of the proposed antenna sensor is carried out using time domain solver in three-dimensional simulation software i.e. Computer Simulation Technology Microwave Studio (CST MWS). Three shapes of ground plane are taken into account, shape-I is the full ground plane structure considered as an initial shape, and then for obtaining the desired results, the shape of the ground plane structure is optimized as presented in shape-II and shape-III. The plot for reflection coefficient magnitude versus resonant frequency is represented in Fig. 1(b) considering the radiating patch having dimensions $6 \times 10 \text{ mm}^2$.

Shape-I has an overall dimension of $10 \times 10 \text{ mm}^2$, shape-II represents a partial ground plane having size $5 \times 10 \text{ mm}^2$, and shape-III shows an asymmetric ground plane with size $7 \times 5.5 \text{ mm}^2$. These structures show different values of reflection coefficients as illustrated in Fig. 1 out of which shape-III shows the most considerable value of reflection coefficient magnitude; therefore, it is chosen for designing the proposed antenna.

Similarly, in Figs 2(a) and 2(b) four different shapes for the radiating patch are considered to optimize patch structure for obtaining desired results. The plot for reflection coefficient magnitude versus resonant frequency is represented in Fig. 2(b) considering the final optimized ground plane structure having dimensions $7 \times 5.5 \text{ mm}^2$.

Shape-I represents the full radiating patch having an overall size $5 \times 10 \text{ mm}^2$, shape-II to shape-IV represent the different shapes of modified radiating patch with various slots etched into the patch. The reflection coefficient magnitude graph for each shape is shown in Fig. 2(b). The reflection coefficient magnitude graph for shape-IV shows the maximum negative value for

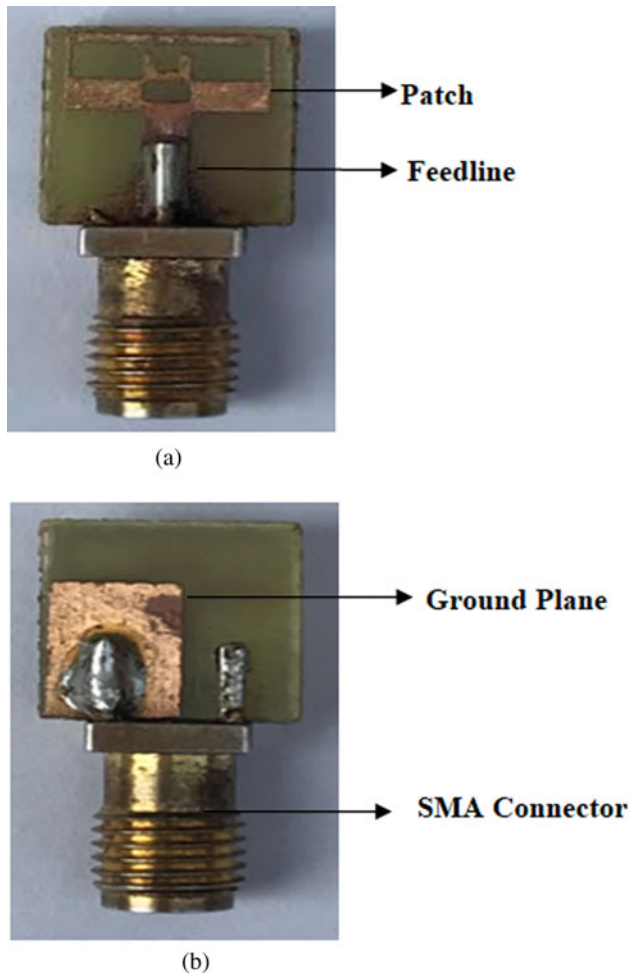


Fig. 4. Photograph of fabricated slot-loaded microstrip line-fed antenna sensor with three-hole SMA connector. (a) Top view. (b) Bottom view.

reflection coefficient magnitude among all other shapes, thus shape-IV is considered as the final shape of radiating patch for the proposed antenna prototype.

Fabrication of proposed antenna sensor

The top and bottom views of the proposed antenna sensor are shown in Fig. 3. The proposed antenna is designed for 50 Ω matching employing FR-4 substrate with thickness = 1.56 mm, relative permittivity (ϵ_r) = 4.4, and loss tangent (δ) = 0.0025 with an overall size of $10 \times 10 \text{ mm}^2$. The position and size of the feedline are optimized to obtain considerably better frequency shift to measure the sensitivity, Q-factor, and accuracy of the antenna. The overall dimensions of substrate, ground plane, radiating patch, and feedline are indicated as $L_s \times W_s$, $L_g \times W_g$, $L_p \times W_p$, and $L_f \times W_f$ respectively. The various slots in the radiating patch are symbolized as S_1 , S_2 , and S_3 . Table 1 represents the values for various geometrical parameters of proposed microstripline-fed antenna sensor.

For the fabrication of proposed antenna sensor, photolithography technique is used, which is based on wet etching method. Wet etching is used to remove unwanted region by immersing the substrate in liquid solution. The top and bottom views of the fabricated sensor with three-hole SMA connector are shown

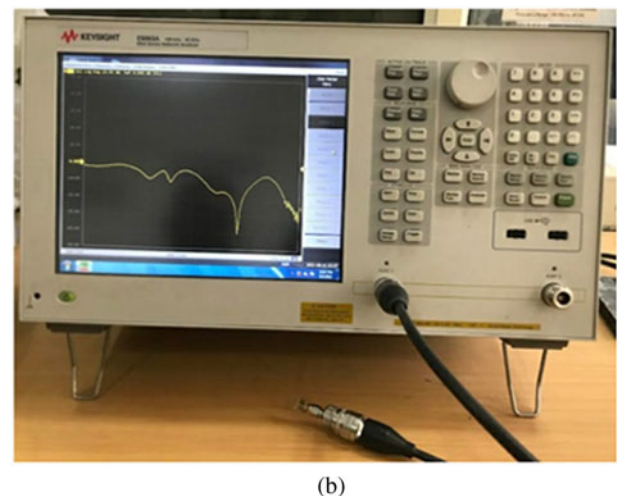
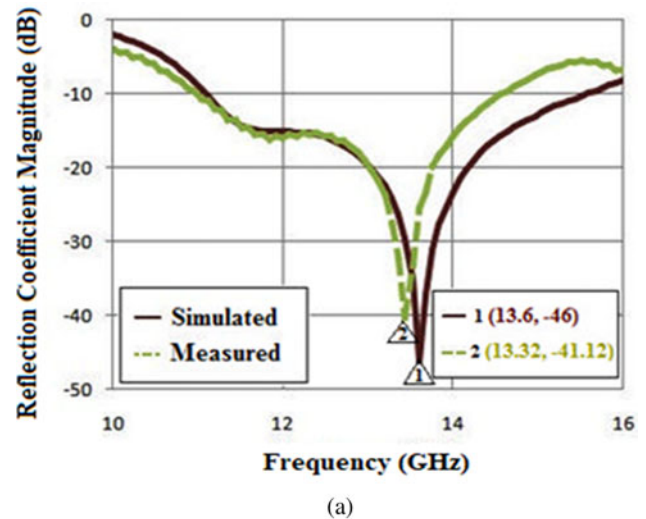


Fig. 5. (a) Simulated and measured response of reflection coefficient magnitude. (b) Reflection coefficient magnitude measurement using Agilent E5071C VNA.

in Fig. 4. The simulated results cover the frequency band from 11.07 to 15.55 GHz with resonant frequency at 13.6 GHz and reflection coefficient magnitude at -46 dB. Further, the measured results show the bandwidth from 11.04 to 14.56 GHz having resonant frequency at 13.32 GHz and reflection coefficient magnitude at -41.12 dB. The experimental results are measured using an Agilent E5071C Vector Network Analyzer (VNA) which shows good agreement with the simulated results indicating good wideband impedance matching with reflection coefficient magnitude under -10 dB. The slightest variation in measured response is due to minor fabrication errors and variation in permittivity of the substrate with frequency. Figure 5 shows the comparison graph of simulated and measured response for reflection coefficient magnitude and photograph of measurement procedure for reflection coefficient magnitude using Agilent E5071C VNA.

The measurement procedure was carried out at Antenna Research Laboratory in Electronics and Communication Engineering Department, Thapar Institute of Engineering and Technology, Patiala, Punjab, India. Further the comparison graphs were plotted using Microsoft Excel 2007.

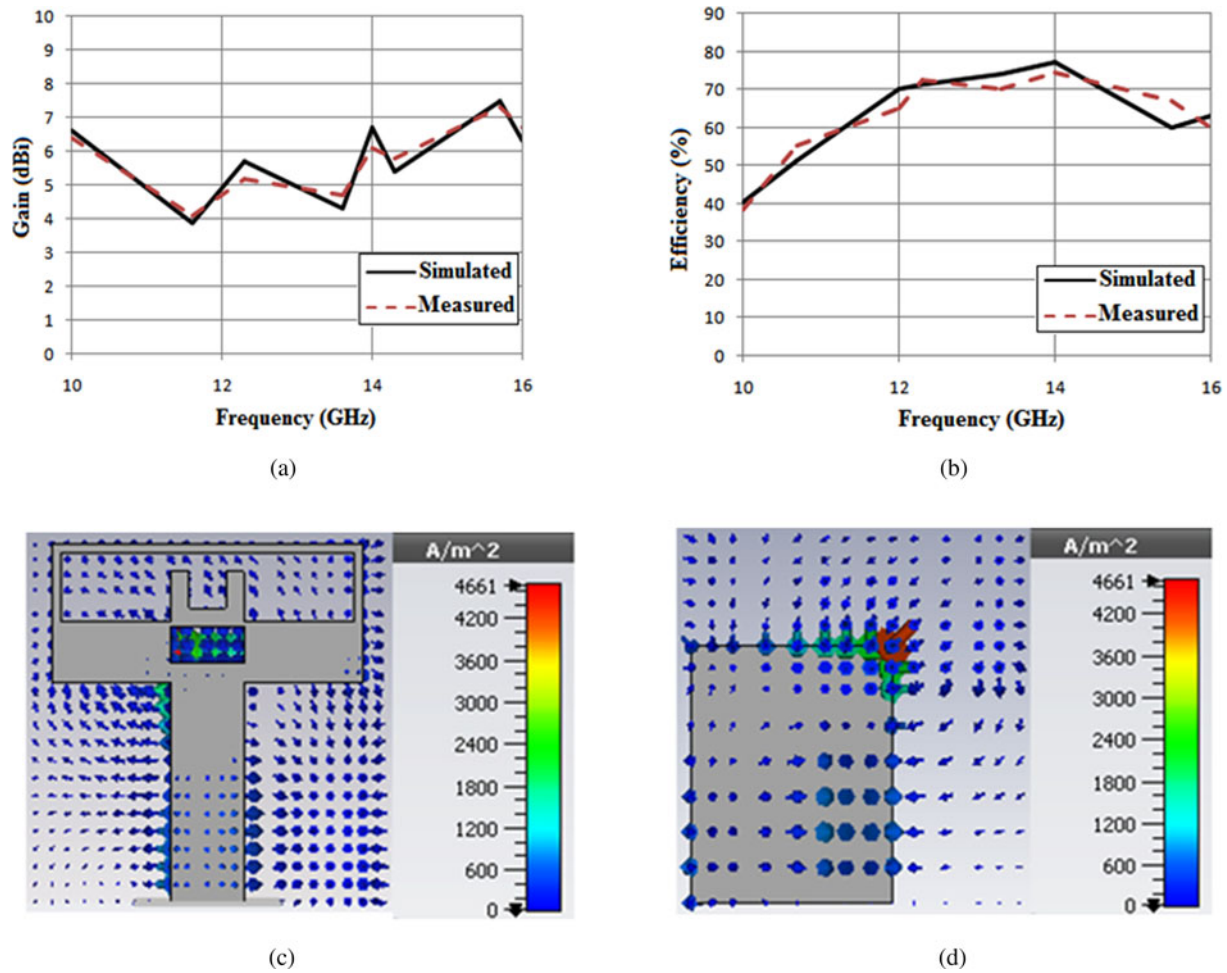


Fig. 6. (a) Comparison graph for simulated and measured gain. (b) Comparison graph for simulated and measured efficiency. (c) Simulated current density on radiating patch. (d) Simulated current density on ground plane of the proposed antenna-based sensor.

Gain, efficiency, and current density of proposed antenna sensor

The measured gain and efficiency of the proposed antenna-based sensor given by VNA are compared with the simulated gain and efficiency given by CST software as illustrated in Figs 6(a) and 6(b). The measured results show a peak gain of 7.58 dBi and an efficiency of 77%, whereas the simulated results show a peak gain of 7.49 dBi and an efficiency of 74%. A close agreement between simulated and measured results is obtained w.r.t. gain and efficiency which proves that the proposed antenna-based sensor is performing accurately. Further, to determine the electromagnetic radiation pattern, current density distribution for the top and bottom view of the proposed antenna-based sensor at 13.32 GHz is analyzed as shown in Figs 6(c) and 6(d). These results show that the slots in the patch and other parameters of the ground plane and feedline are solely liable for bandwidth enhancement and overall appreciable performance of radiation characteristics of the proposed antenna-based sensor.

Sensitivity, Q-factor, and accuracy of proposed antenna sensor

The proposed sensor significantly shows the high sensitivity of 280 MHz as a frequency function. In order to compute the sensitivity of the proposed antenna sensor as a function of frequency, shift in resonant frequency (Δf) of the input reflection coefficient magnitude is measured w.r.t. the simulated and measured results

of the proposed antenna sensor. Here the simulated and measured results are considered under unloaded conditions i.e. when we are not testing any samples.

The quality factor for the proposed antenna-based sensor is calculated as 409. Based on the resonant frequency and bandwidth of the resonator the Q-factor of the antenna can be calculated as: [32]

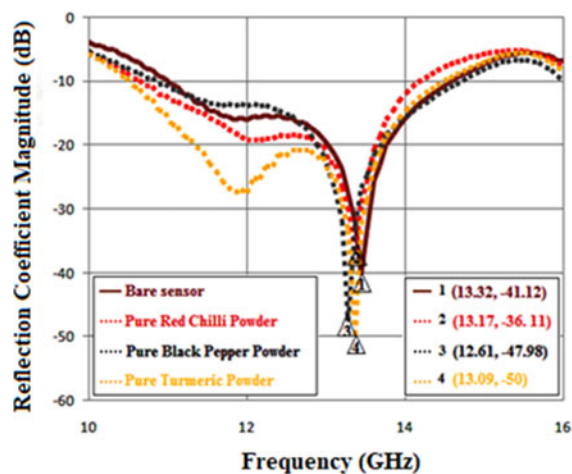
$$Q - \text{factor} = f_r / BW, \quad (1)$$

where f_r is the resonant frequency and BW is the bandwidth of the resonator.

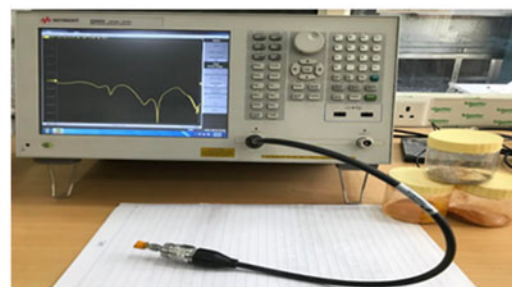
Further, higher sensitivity gives greater accuracy in measurement as a small change in real part of the permittivity can be measured easily. The proposed antenna-based sensor shows 98% accuracy, which proves that the proposed sensor could be utilized for food adulteration-detecting application.

The proposed antenna-based sensor for solid food evaluation

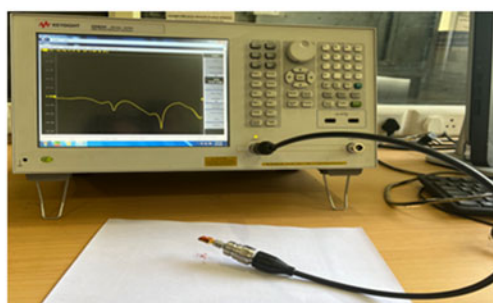
In this section, the capability of the proposed antenna-based sensor is checked for solid food evaluation. Firstly raw spices, i.e. red chilli powder, black pepper powder, and turmeric powder, were considered as pure sample. Two grams (0.002 kg) each of pure



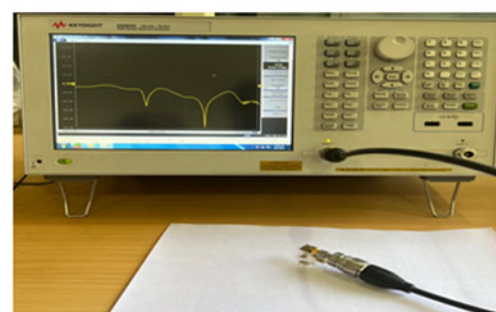
(a)



(b)



(c)



(d)

Fig. 7. (a) Measured reflection coefficient magnitude response for the proposed sensor loaded with all pure samples of red chilli, black pepper, and turmeric powder. (b, c) Experimental setup during measurement with samples loaded on the surface of the proposed antenna sensor.

sample were measured with weighing machine and are kept on top of the antenna-based sensor for about 2 min. It is found that the process becomes stable at approximately 2 min after keeping the sample on the radiating patch. The reflection coefficient magnitude for pure samples of spices is measured using VNA; the average of five readings is taken from the large set of experiments that were observed for about 20 times. This same procedure is opted for each pure sample of spices after a gap of 10 min. After this, a binary mixture is prepared by adding different adulterants with pure samples for analyzing different cases: (i) red chilli powder adulterated with brick powder; (ii) black pepper powder adulterated with papaya seeds powder; and (iii) turmeric powder with artificial yellow color. The mixture is prepared by weight which is measured using a weighing machine; all samples of equal weight are then separately tested and reflection coefficient magnitude response with respect to frequency shift for each case is measured using VNA and represented in graphical form. The average of five values for each adulterated spice sample was taken that was observed up to 20 times. All the measurements were taken at room temperature (25°C), and after each measurement, the sensor was washed with water and wiped with tissue paper. Finally, a comparison graph was plotted from the results obtained for unadulterated sample and adulterated sample mixture at different adulteration levels. The phenomenon associated with resonant frequency shift is dielectric perturbation and change in reflection coefficient magnitude is due to the solid's response to

electromagnetic radiation, which depends upon the properties of material, temperature, and chemical composition.

The measured reflection coefficient magnitude graph with respect to resonant frequency for all pure spice samples is plotted in Fig. 7(a) and photographs depicting the measurements with samples loaded on the surface of the proposed antenna sensor are shown in Figs 7(b) and 7(c). Figure 7(a) represents that the proposed sensor loaded with a pure sample of red chilli powder, black pepper powder, and turmeric powder resonates at 13.17, 12.61, and 13.09 GHz with reflection coefficient magnitude at -36.11, -47.98, and -50 dB respectively, whereas the unloaded sensor resonates at 13.32 GHz with -41.12 reflection coefficient.

Sensitivity and dielectric permittivity analysis

The experimental results of the proposed antenna-based sensor w.r.t. pure spice samples (red chilli, black pepper, and turmeric powder) show considerably good sensitivity and measured dielectric permittivity values are illustrated in Table 2. As the proposed antenna sensor has good accuracy, it can detect even a small change in the dielectric permittivity of different materials. As shown in Fig. 8, the antenna sensor is examined for different permittivity values w.r.t. resonant frequency, the relationship between the resonant frequency and different values of dielectric permittivity illustrates that as the value of dielectric permittivity increases, resonant frequency decreases and vice versa. Thus this proves that the proposed antenna sensor is a valid tool for

Table 2. Measured values of sensitivity and dielectric permittivity for the proposed antenna-based sensor w.r.t. resonant frequency and reflection coefficient

Sample material	Resonant frequency (GHz)	Reflection coefficient (dB)	Measured permittivity	Sensitivity (MHz)
Pure red chilli powder	13.17	-36.11	15.30	150
Pure black pepper powder	12.61	-50	26.70	710
Pure turmeric powder	13.09	-47.98	17.19	230

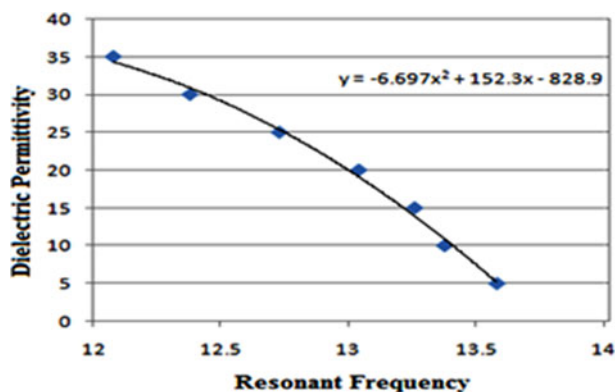


Fig. 8. Relationship between resonant frequency and dielectric permittivity.

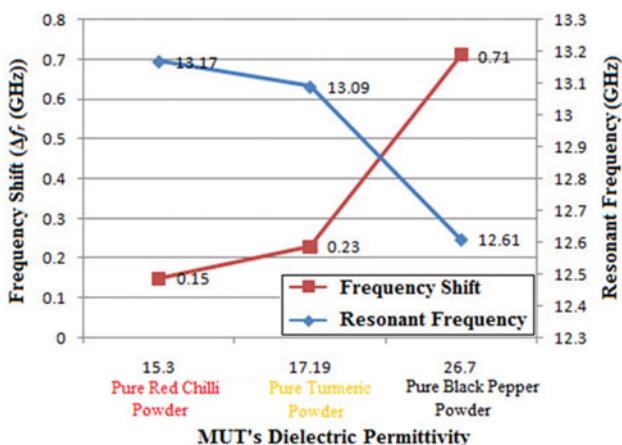


Fig. 9. Relationship between frequency shift, resonant frequency, and measured dielectric permittivity of pure spice samples (red chilli, black pepper, and turmeric powder).

detecting adulteration in food materials having different dielectric permittivity values. The mathematical expression for measured dielectric permittivity of tested samples is obtained as: [33]

$$\epsilon_r = -6.697f_r^2 + 152.3f_r - 828.9.$$

Figure 9 shows the relationship between the resonant frequency and measured dielectric permittivity. This graph depicts that as the resonant frequency increases, the dielectric permittivity of the pure spice samples decreases depending upon material properties.

Estimation of adulteration

For estimating the adulteration, testing on pure samples is carried out to check the accuracy and sensitivity of the proposed antenna sensor.

Table 3. LOD in different spice samples

S. No.	Adulterant	Quantity of adulterants (g)
1.	Brick powder	0.05
2.	Papaya seeds powder	0.05
3.	Artificial yellow color	0.05

Table 4. Experimental data of MUT

Brick powder in red pure red chilli (g)	Resonant frequency (GHz)	Shift in f_r (GHz)	Measured dielectric permittivity
0.05	11.43	1.74	36.96
0.1	10.90	2.27	35.5
0.15	10.78	2.3	34.65
0.2	10.86	2.33	35.23

Therefore, various adulterants such as brick powder, papaya seeds powder, and artificial yellow color are mixed with a pure sample of red chilli, black pepper, and turmeric powder separately. The change in reflection coefficient magnitude and resonant frequency is observed on mixing the adulterant into the pure sample and this change occurs according to the level of adulterant added to the pure samples [34]. Further, the sensitivity performance of the proposed antenna sensor as a function of frequency is measured w.r.t. shift in resonant frequency (Δf (MHz)) of the input reflection coefficient magnitude as 150, 710, and 230 MHz for red chilli, black pepper, and turmeric powder respectively using the formula:

$$\Delta f = f_{ru} - f_{rl}, \tag{2}$$

where f_{ru} is the resonant frequency of the proposed antenna sensor for unloaded condition and f_{rl} is the resonant frequency of the proposed antenna sensor for loaded condition.

In this section, the limit of detection (LOD) was estimated for various adulterants added to pure spice's samples as illustrated in Table 3. For this study, three different binary mixtures were prepared with different quantities of adulterants to check adulteration at various levels. Pure spices were considered as reference sample to analyze the adulteration procedure.

Case (i): red chilli powder adulterated with brick powder. Red chilli powder is one of the most common spices used in Indian kitchen for enhancing the color of the dish and also used as a tempering spice. However, red chilli is usually adulterated with brick powder to add weight and bright red color to it; hence, it

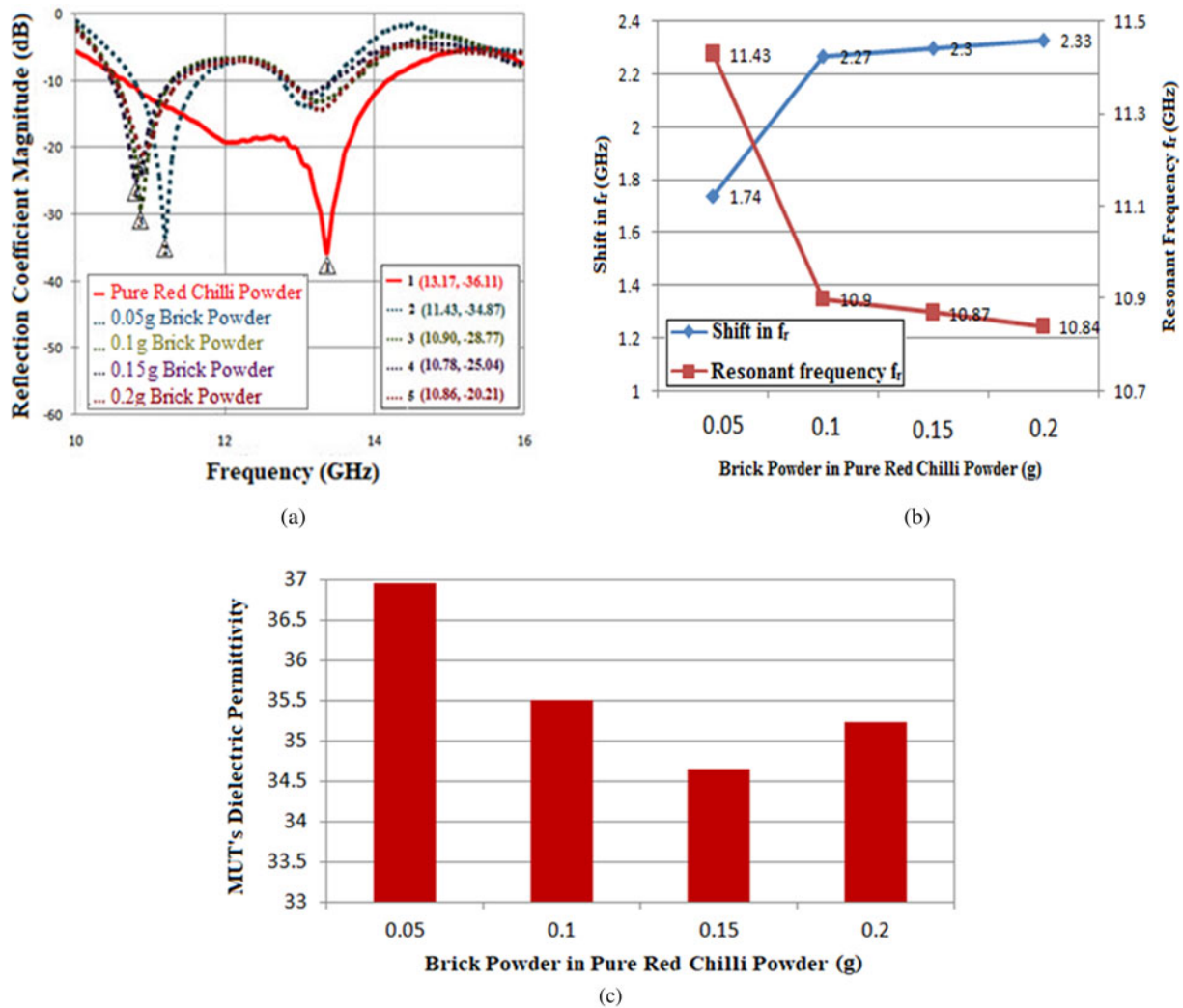


Fig. 10. (a) Measured reflection coefficient magnitude with respect to resonant frequency for pure red chilli powder adulterated with brick powder at different levels of adulteration. (b) Relationship between shift in frequency and resonant frequency (f_r) at different levels of adulteration in pure red chilli powder. (c) Measured dielectric permittivity of the MUT corresponding to the amount of the adulterant in pure sample.

is very dangerous to health if consumed on regular basis. For this case study, four different samples were prepared by mixing brick powder with red chilli powder in different concentrations of adulterant. Keeping the total weight 0.2 g, binary mixtures were prepared, starting with 0.2 g considered as a pure red chilli sample and 0 g brick powder (adulterant), then gradually adding 0.05 g brick powder to 0.15 g pure red chilli powder, so that the total weight remains 0.2 g. At last 0.2 g of brick powder is considered as a pure adulterated sample with 0 g red chilli powder (unadulterated) mixed in it. Table 4 represents the experimental data of red chilli powder adulterated with brick powder.

Figure 10(a) shows the reflection coefficient magnitude with respect to resonant frequency for pure red chilli powder when mixed with brick powder at different levels of adulteration. The reflection coefficient magnitude for pure red chilli which is considered as a reference sample is -36.11 dB at 13.17 GHz resonant frequency, whereas the reflection coefficient magnitude for brick powder when 0.05 , 0.1 , 0.15 , and 0.2 g mixed with pure sample is -34.87 , -28.77 , -25.04 , and -20.21 dB resonating at 11.43 , 10.90 , 10.78 , and 10.86 GHz respectively. This graph illustrates that as the level of adulteration increases the corresponding

reflection coefficient magnitude decreases due to change in dielectric properties of the material which further results in shift of resonant frequencies. Figure 10(b) shows the relationship between shift in frequency and resonant frequency (f_r) at different levels of adulteration in pure red chilli powder. Further, Fig. 10(c) represents the measured dielectric permittivity of the MUT i.e. brick powder in pure red chilli powder corresponding to the amount of adulterant in pure sample.

Case (ii): black pepper powder adulterated with papaya seeds powder. Black pepper powder is usually adulterated with papaya seeds powder to add bulk to the material. In this section, four different adulteration levels were prepared from 0.05 to -0.2 g by mixing papaya seeds powder in pure black pepper powder, considering 0.2 g of papaya seeds as a pure adulterated sample with 0 g black paper powder. As the concentration of adulterant increases the dielectric permittivity of the MUT changes, which results in change of reflection coefficient magnitude and resonant frequency. Table 5 represents the experimental data of black pepper powder adulterated with papaya seeds powder.

Table 5. Experimental data of MUT

Papaya seeds powder in black pepper powder (g)	Resonant frequency (GHz)	Shift in f_r (GHz)	Measured dielectric permittivity
0.05	11.29	1.32	36.94
0.1	11.27	1.34	36.92
0.15	11.10	1.51	36.5
0.2	10.82	1.79	34.95

These changes are illustrated in Fig. 11(a) w.r.t. pure black pepper powder which is considered as a reference sample. The reflection coefficient magnitude for pure black pepper powder is -47.98 dB with resonant frequency at 12.61 , whereas the reflection coefficient magnitude for papaya seeds powder mixed with pure black pepper powder is -40.02 , -33.14 , -27.98 , and -22.38 dB for 0.05 , 0.1 , 0.15 , and 0.2 g quality of adulterant having a resonant frequency at 11.29 , 11.27 , 11.10 , and 10.82 GHz respectively. As the level of adulteration increases in the pure sample, reflection coefficient magnitude decreases with shift in resonant frequency owing to change in dielectric permittivity of the

mixture. Further, Fig. 11(b) shows the relationship between shift in frequency and resonant frequency (f_r) when pure sample is adulterated with different levels of adulteration. Further, Fig. 11(c) represents the measured dielectric permittivity of the MUT, i.e. black pepper powder adulterated with papaya seeds powder corresponding to the amount of adulterant in pure sample.

Case (iii): turmeric powder adulterated with artificial yellow color. Turmeric is a yellow-colored spice with many health benefits; however, it is adulterated with artificial yellow color to increase the amount of turmeric powder. Similar procedure is chosen here to study the adulteration in turmeric powder, with different volumes of artificial yellow color mixed with pure sample. Figure 12(a) shows the variation in reflection coefficient magnitude and shift in resonant frequency w.r.t. different adulteration levels in pure sample where 0.2 g is considered as an adulterated sample with no amount of pure turmeric powder added to it. Pure turmeric powder is considered as a reference sample, having reflection coefficient magnitude -50 dB and resonant frequency 13.09 GHz. Table 6 represents the experimental data of black pepper powder adulterated with papaya seeds powder.

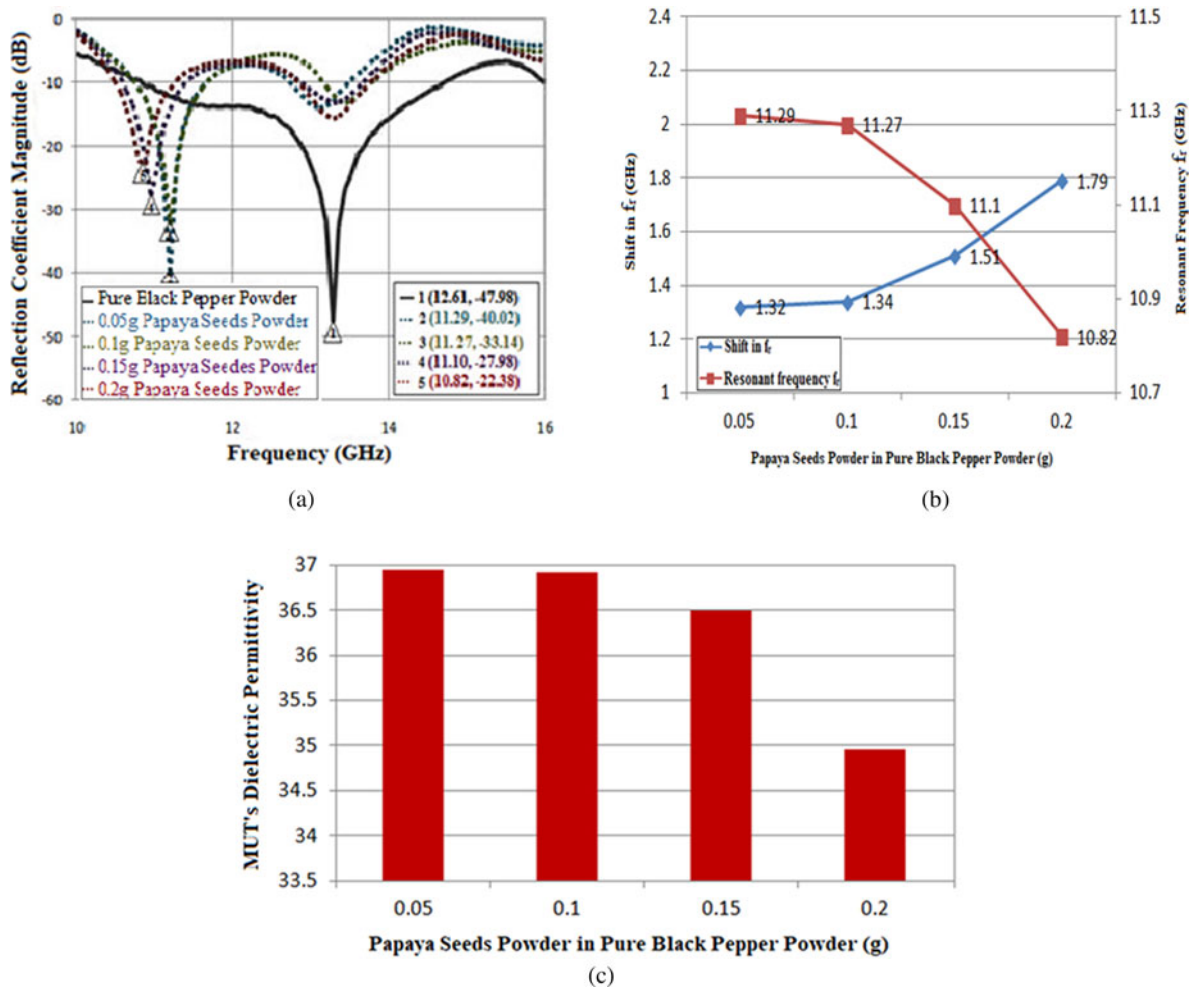


Fig. 11. (a) Measured reflection coefficient magnitude with respect to resonant frequency for pure black pepper powder adulterated with papaya seeds powder at different levels of adulteration. (b) Relationship between shift in resonant frequency and resonant frequency (f_r) at different levels of adulteration in pure black pepper powder. (c) Measured dielectric permittivity of the MUT corresponding to the amount of the adulterant in pure sample.

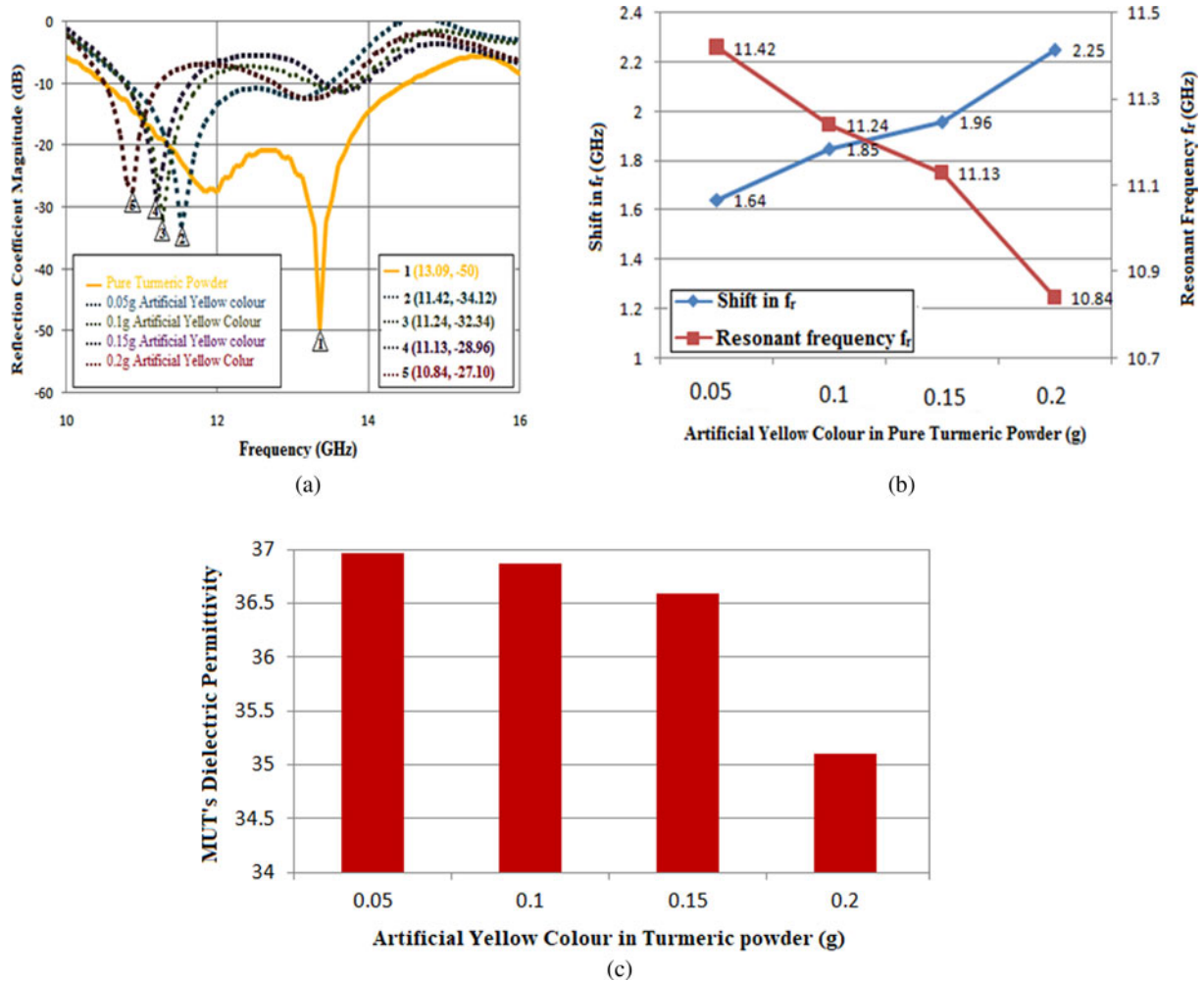


Fig. 12. (a) Measured reflection coefficient magnitude with respect to resonant frequency for pure turmeric powder adulterated with artificial yellow powder at different levels of adulteration. (b) Relationship between shift in frequency and resonant frequency (f_r) at different levels of adulteration in pure turmeric powder. (c) Measured dielectric permittivity of the MUT corresponding to the amount of the adulterant in pure sample.

Table 6. Experimental data of MUT

Artificial yellow color in turmeric powder (g)	Resonant frequency (GHz)	Shift in f_r (GHz)	Measured dielectric permittivity
0.05	11.42	1.64	36.97
0.1	11.24	1.85	36.87
0.15	11.13	1.96	36.59
0.2	10.84	2.25	35.1

The reflection coefficient magnitude for adulterated sample at 0.05, 0.1, 0.15, and 0.2 g is -34.12 , -32.34 , -28.96 , and -27.10 dB having resonant frequency at 11.42, 11.24, 11.13, and 10.84 GHz respectively. Figure 12(b) shows the relationship between shift in frequency and resonant frequency (f_r) when pure sample is adulterated with different levels of adulteration. These results illustrate that as the concentration of adulterant increases in the pure sample, reflection coefficient magnitude decreases with shift in resonant frequency which is due to the change in

dielectric properties of the MUT. Further, Fig. 12(c) represents the measured dielectric permittivity of the MUT, i.e. turmeric powder adulterated with artificial yellow color corresponding to the amount of adulterant in pure sample.

Figure 13 depicts the variation in reflection coefficient magnitude for various pure spice samples with different adulterants at different adulteration levels.

Results and discussion

The methodology instigated for this work is based on the interaction of electromagnetic field owing to shift in resonant frequency and change in reflection coefficient magnitude as a function of dielectric permittivity of the sample which supports the detection of adulteration in food materials. All the above experimental results illustrate that the composition of the solution changes as well as the degree of saturation, when the level of adulteration increases which results in change of dielectric properties of the binary mixture, whose effect can be observed in the variation of reflection coefficient magnitude and in resonant frequency shift. The variability of the reflection coefficient magnitude at different levels of adulteration depends upon the

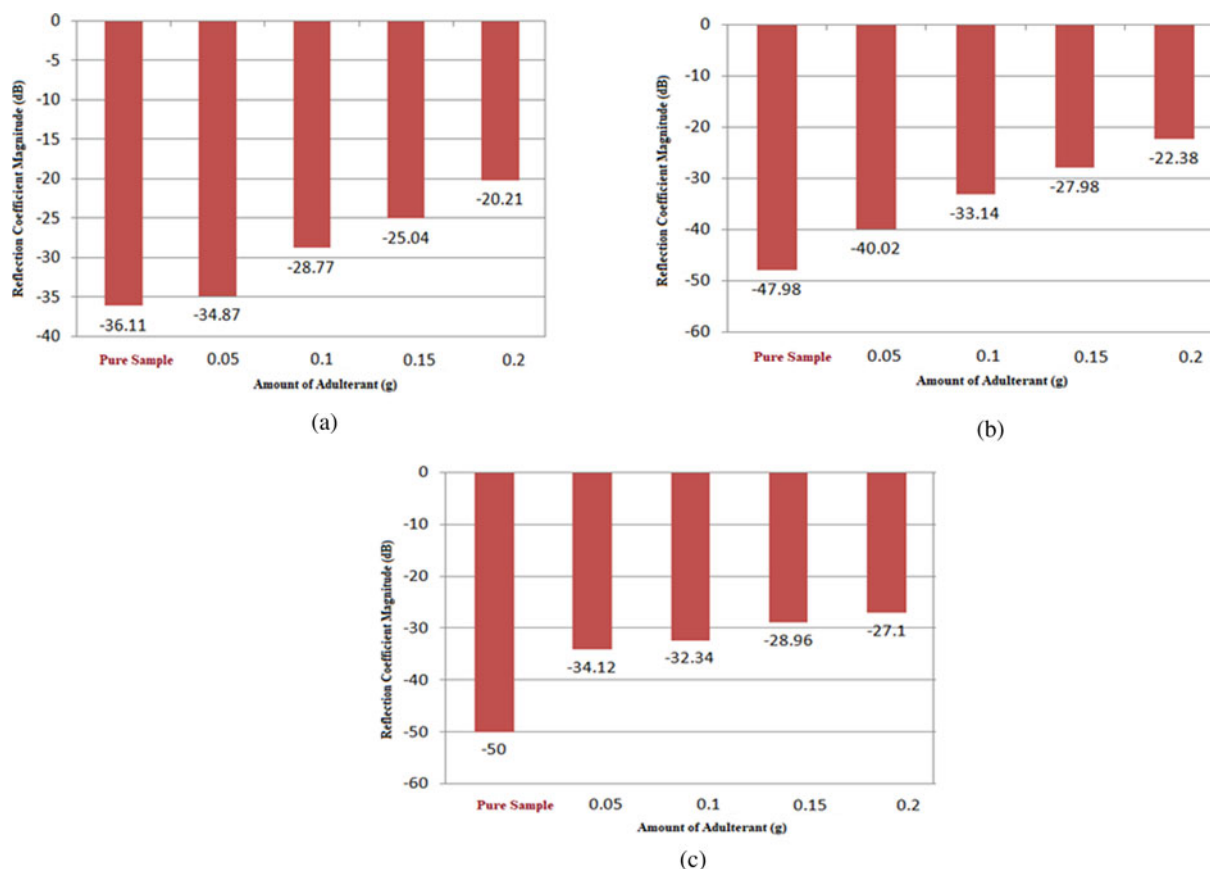


Fig. 13. Variation in reflection coefficient magnitude at 0.05, 0.1, 0.15, and 0.2 g amount of adulterant for (a) red chilli powder adulterated with brick powder, (b) black pepper powder adulterated with papaya seeds powder, (c) turmeric powder adulterated with artificial yellow color.

dielectric permittivity of the material, which increases or decreases depending upon the type of adulterant and its concentration level in the mixture. For instance, the dielectric permittivity of the mixture decreases with an increase in the percentage of adulteration in the pure sample; as a result, reflection coefficient magnitude also decreases and vice versa. Figure 13 depicts the variation in reflection coefficient magnitude for all pure samples that are adulterated with different adulterants at 0.05, 0.1, 0.15, and 0.2 g amount of adulteration.

It is observed from the aforementioned results that as the level of adulteration increases the dielectric permittivity of the material decreases which results in a decrease of reflection coefficient magnitude w.r.t. shift in resonant frequency.

The validation data of reproducibility for some common spice's adulteration are illustrated in Table 7. Other figures of merits for the proposed slot-loaded microstrip line-fed antenna-based sensor, such as LOD, sensitivity, accuracy, and Q-factor, prove it to be a valid tool for detecting adulteration in solid food without deteriorating the quality of the food. Further, it gives high coefficient of determination ($R^2 > 0.343$) which is used to predict dielectric permittivity of the MUT and has standard deviation less than the difference between unadulterated and adulterated values, giving resolution high enough to distinguish adulteration with an acceptable statistical accuracy. Moreover, it does not require any harmful chemicals or expensive equipment, thus reducing its complexity and making it a cost-effective device for monitoring food quality. A single sensor is used for performing experiments from January 2022 to February 2021. All the

Table 7. Reproducibility data for some common adulterants in spices

S. No.	Adulterant	Reproducibility (RSD %)
1.	Brick powder	22
2.	Papaya seeds powder	24
3.	Artificial yellow color	17

experimental results obtained after a number of trails were plotted in graphs herein. The results start to degrade as the number of trails increases; this may be due to some material sticking to the radiating patch. However, if we calibrate the sensor carefully, wash and wipe it properly after each experiment, this will not affect the measurement. Further, it is observed that this sensor is sustainable for about 1000 trails, after that the pattern on the substrate starts to peel off and become faded that degrades the performance of the sensor. The shelf life of this antenna-based sensor is approximately more than 1 year.

Few things that are appreciable about the proposed sensor owing to its high sensitivity and Q-factor are:

1. This sensor is capable of detecting very small amount of adulterant since its LOD is 0.05 g. The proposed sensor is capable of detecting each constituent separately providing sufficient range between their frequency shift and reflection coefficient magnitude that helps in analyzing adulteration for different levels of adulterants.

Table 8. A detailed comparison with earlier reported work in terms of the analytical performance

References	Size of sensor (mm ²)	Operating frequency (GHz)	Sample tested	Q-factor	Sensitivity (%)	Accuracy (%)	Limit of detection	Sensor structure
[8]	68.12 × 38.69	3.98	Solid	174	–	92.5	–	RRR
[11]	35 × 25	2.45	Water	45	21.4	95	2.65 µl	MCSRR
[13]	40 × 26	2.65	Solid	80	–	97	–	CSRR
[17]	50 × 50	2.45	Liquid and paste	154.4	1.5	0.4	–	SMRR
[21]	–	1.85	Liquid or solid	–	7.4	91.66	–	Double SRR
[22]	50 × 30	2.45	Solid	–	0.25	94	–	IDC-SSR
[29]	40 × 20	2.074	Glucose	–	–	98.59	700 ng, 400 ng	ENG resonator
[31]	53 × 53	2.44	Oil	146	1.33	98.47	–	VSRR
[35]	–	3.9	Flours	–	11.6	–	µg	Electric-LC resonator
This work	10 × 10	13.32	Spices	409	28	98	0.5 g	Microstrip antenna

2. It helps to detect the adulteration for unknown permittivity materials as well as for materials having high permittivity.

However, it is observed from the measurement procedure that though the proposed slot-loaded microstrip line-fed antenna-based sensor is capable of detecting different levels of adulteration, it is incapable to identify the kind of adulterant present in the sample, reporting it as a drawback of this sensor. A detailed comparison with earlier reported work in terms of the analytical performance is depicted in Table 8.

Conclusions

In this work, a miniature slot-loaded microstripline-fed antenna-based sensor is investigated for detecting adulteration in red chilli powder adulterated with brick powder, black pepper powder adulterated with papaya seeds powder, and turmeric powder with artificial yellow color. The protocol was designed and fabricated on an inexpensive FR-4 substrate with thickness = 1.56 mm and permittivity (ϵ_r) = 4.4 having reflection coefficient magnitude -41.21 dB at 13.32 GHz resonant frequency. The simulated and measured results considerably show good agreement, which validates the proposed antenna sensor for detecting adulteration in spices with high sensitivity. The proposed sensor has a Q-factor of 409, showing significantly high sensitivity of 280 MHz with 98% accuracy. Further, the proposed antenna sensor has high repeatability due to small value of standard deviation for measured results. The experimental procedure of this proposed sensor is based upon the interaction of the sample food materials with the electromagnetic field owing to shift in resonant frequency as a function of dielectric permittivity of the samples. This sensor has certain LOD; however, it could detect low permittivity materials also. The proposed sensor does not need any harmful chemicals or expensive equipment and it has less performance time with easy data interpretation. The results of this study recommend that the proposed antenna-based sensor with novel configuration can be used for industrial purposes as it is having a relatively less

complex procedure for determining the extent of adulteration in solid food materials with high accuracy.

For future examination, more variety of materials like fuel, oil, etc., can be investigated for detecting adulteration using such antenna-based sensors with more compact size.

Acknowledgements. The authors are highly grateful to TIET-VT Centre of Excellence for Emerging Materials (CEEMS) for their support in funding this project. We would also like to thank Hitendra, Ph.D. Scholar, Antenna Research Lab, ECEDat TIET and Amanpreet Singh, Lab Technician, Capstone Lab, ECED at TIET for their assistance in antenna measurements. We also thank Arianz India Pvt. Ltd. Mohali, Punjab, India for the smooth and timely fabrication of our proposed antenna.

Conflict of interest. None.

Ethical standards. On behalf of all co-authors, I, Nitika, declare that this article has not been published in or is not under consideration for publication elsewhere. All authors were actively involved in the work leading to the manuscript and will hold themselves jointly and individually responsible for its content. Also, there is no conflict of interest in this paper.

References

1. Bansal S, Singh A, Mangal M, Mangal AK and Kumar S (2017) Food adulteration: sources, health risks, and detection methods. *Critical Reviews in Food Science and Nutrition* 57, 1174–1189.
2. Awasthi S, Jain K, Das A and Alam R (2014) Analysis of food quality and food adulterants from different departmental & local grocery stores by qualitative analysis for food safety. *IOSR – Journal of Environmental Science, Toxicology and Food Technology* 8, 22–26.
3. Mohammad AM, Chowdhury T, Biswas B and Absar N (2018) Food poisoning and intoxication: a global leading concern for human health. In Grumezescu AM and Holban AM (eds), *Food Safety and Preservation: Modern Biological Approaches to Improving Consumer Health*. Amsterdam: Elsevier science, pp. 307–352.
4. Choudhary A, Gupta N, Hameed F and Choton S (2020) An overview of food adulteration: concept, sources, impact, challenges and detection. *International Journal of Chemical Studies* 8, 2564–2573.
5. Ades G, Henry CW and Feldstein F (2012) The food safety challenge of the global food supply chain. *WEBINARS, Food saf Mag.*

6. **Ayza A and Belete E** (2015) Food adulteration: its challenges and impacts. *Food Science and Quality Management* **41**, 50–57.
7. **Alauddin S** (2012) Food adulteration and society. *Global Journal for Research Analysis* **1**, 3–5.
8. **Alahnomi R, Hamid NBA, Zakaria Z, Sutikno T, Azuan A and Bahar M** (2018) Microwave planar sensor for permittivity determination of dielectric materials. *Indonesian Journal of Electrical Engineering and Computer Science* **11**, 362–371.
9. **Weng YK, Chen J, Cheng CW and Chen C** (2020) Use of modern regression analysis in the dielectric properties of foods. *Foods* **9**.
10. **Zajicek R and Vrba J** (2010) Broadband complex permittivity determination for biomedical applications. *Advanced Micro Circuits and Systems*, 365–385.
11. **Javed A, Arif A and Zubair M** (2020) A low-cost multiple complementary split-ring resonator based microwave sensor for contactless dielectric characterization of liquids. *IEEE Sensors Journal* **20**, 11326–11334.
12. **Posudin Y, Peiris K and Kays S** (2015) Non-destructive detection of food adulteration to guarantee human health and safety. *Ukrainian Food Journal* **4**, 207–260.
13. **Ansari MAH, Jha AK and Akhtar MJ** (2015) Design and application of the CSRR-based planar sensor for noninvasive measurement of complex permittivity. *IEEE Sensors Journal* **15**, 7181–7189.
14. **Jain S, Mishra PK, Thakare VV and Mishra J** (2018) Microstrip moisture sensor based on microstrip patch antenna. *Progress in Electromagnetics Research M* **76**, 177–185.
15. **Menon AKI, Pranav S, Govind S and Madhu Y** (2020) RF sensor for food adulteration detection. *Progress in Electromagnetics Research Letters* **9**, 137–142.
16. **Rajendran J, Menon SK and Donelli M** (2020) A novel liquid adulteration sensor based on a self complementary antenna. *Progress in Electromagnetics Research C* **103**, 97–110.
17. **Kunte AA and Gaikwad AN** (2018) Dielectric constant measurement of low loss liquids using stacked multi ring resonator. *Sadhana* **43**, 2–112.
18. **Tiwari NK, Singh SP, Mondal D and Akhtar MJ** (2019) Flexible biomedical RF sensors to quantify the purity of medical grade glycerol and glucose concentrations. *International Journal of Microwave and Wireless Technologies* **12**, 1–11.
19. **Nitika, Jaswinder K and Khanna R** (2021) Novel monkey-wrench-shaped microstrip patch sensor for food evaluation and analysis. *Journal of the Science of Food and Agriculture*.
20. **Alahnomi RA, Zakaria Z, Yussof ZM, Althuwayb AA, Alhegazi A, Alsariera H and Rahman NA** (2021) Review of recent microwave planar resonator-based sensors: techniques of complex permittivity extraction, applications, open challenges and future research directions. *Sensors* **21**, 1–38.
21. **Romera GG, Herraiz-Martínez FJ, Martínez-Martínez JJ and Gil M** (2016) Submersible printed split-ring resonator-based sensor for thin-film detection and permittivity characterization. *IEEE Sensors Journal* **16**, 1–1.
22. **Muhammed Shafi KT** (2017) Improved planar resonant RF sensor for retrieval of permittivity and permeability of materials. *IEEE Sensors Journal* **17**, 5479–5486.
23. **Rahman MN, Islam MT and Samsuzzaman M** (2018) Development of a microstrip-based sensor aimed at salinity and sugar detection in water considering dielectric properties. *Microwave and Optical Technology Letters* **60**, 667–672.
24. **Zajicek R, Smejkal T, Oppl L and Vrba J** (2008) Broadband measurement of complex permittivity using reflection method and coaxial probes. *Radioengineering* **17**, 14–19.
25. **Abbas Z, Hashim M, Mokhtar R and Aziz S** (2007) RDWG technique of determination of moisture content in oil palm fruits. *EPJ Applied Physics* **40**, 207–210.
26. **Manzari S, Occhiuzzi C, Nawale S and Catini A** (2012) Humidity sensing by polymer-loaded UHF RFID antennas. *IEEE Sensors Journal* **12**, 2851–2858.
27. **Hichmen A, Ghodbane H, Amir M, Zidane MA, Hamouda C and Rouane A** (2020) Microstrip sensor for product quality monitoring. *Journal of Computational Electronics* **19**, 1329–1336.
28. **Arroyo NMA, Wrobel K, Aguilar AFJ, Barrientos YE, Escobosa CAR and Wrobel K** (2018) Determination of fatty acid methyl esters in cosmetic castor oils by flow injection electrospray ionization high-resolution mass spectrometry. *International Journal of Cosmetic Science* **40**, 295–302.
29. **Kumari R, Patel PN and Yadav R** (2018) An ENG resonator-based microwave sensor for the characterization of aqueous glucose. *Journal of Physics D: Applied Physics* **51**, 1–17.
30. **Meng Z, Wu Z and Gray J** (2017) Microwave sensor technologies for food evaluation and analysis: methods, challenges and solutions. *Transactions of the Institute of Measurement and Control* **40**, 3433–3448.
31. **Kulkarni S and Joshi MS** (2015) Design and analysis of shielded vertically stacked ring resonator as complex permittivity sensor for petroleum oils. *IEEE Transactions on Microwave Theory and Techniques* **63**, 2411–2417.
32. **Azaryan NS, Batouritski MA, Budagov YA, Demyanov SE, Karpovich VV, Liubetski NV, Maximov SI, Rodionova VN and Shirkov GD** (2018) Measurement of high values of Q-factor of 1.3 GHz superconducting cavity of TESLA-type. *Universal Journal of Materials Science* **6**, 1–7.
33. **Alhegazi A, Zakaria Z, Shairi NZ, Sutikno T, Alahnomi RA and Abu-Khadrah AI** (2019) Analysis and investigation of a novel microwave sensor with high Q-factor for liquid characterization. *TELKOMNIKA* **17**, 1065–1070.
34. **Chakraborty M and Biswas K** (2018) Limit of detection for five common adulterants in milk: a study with different fat percent. *IEEE Sensors Journal* **18**, 2395–2403.
35. **Varshney PK, Sharma A and Akhtar MJ** (2019) Exploration of adulteration in some food materials using high-sensitivity configuration of electric-LC resonator sensor. *International Journal of RF and Microwave Computer-Aided Engineering* **30**, 1–9.



Nitika received her Bachelor of Technology in Electronics and Communication Engineering from Chandigarh Group of Colleges, Mohali, India in 2015 and Masters of Engineering in Wireless Communication from T.I.E.T., Patiala, Punjab, India in 2017. Presently, she is pursuing Ph.D. from T.I.E.T., Patiala. Her research interests emphasize on design and optimization of microstrip patch antennas using optimization algorithms such as differential evolution (DE) algorithm, genetic algorithm (GA), and particle swarm optimization (PSO) algorithm. Her research interest also includes detecting adulteration in food materials.



Jaswinder Kaur received her Bachelor of Technology and Master of Technology in Electronics and Communication Engineering from Punjab Technical University, Jalandhar, Punjab, India in 2005 and 2009, respectively. She received her Ph.D. degree from Thapar University, Patiala, Punjab, India in 2014. Presently, she is working as an Assistant Professor in the Department of Electronics and Communication Engineering, Thapar Institute of Engineering and Technology (T.I.E.T.), Patiala, Punjab, India. She has published several papers in various peer-reviewed journals/conferences of national and international repute. Her research interests include the analysis and design of microstrip patch antennas for wireless communication, 5G MIMO antenna, CSRRs, flexible antennas, and antennas for biomedical applications.



Rajesh Khanna received his B.Sc. (Engg.) degree in Electronics and Communication in 1988 from Regional Engineering College, Kurukshetra, Haryana, India, and M.E. degree in 1998 from Indian Institute of Sciences, Bangalore, India. Presently, he is working as a Professor and Head of the Department of Electronics and Communication, Thapar University, Patiala, Punjab, India. He has published 80 papers in national and international journals/conferences. He has research projects worth Rs 1.5 crores to his credit. His research interests include the analysis and design of antennas, wireless communication, multiple input multiple output (MIMO), and fractional Fourier transform-based wireless.